Thermodynamic modelling of the V-Ti-B system

M. Yazlak[1]*, H.-J. Christ[1], W. Yang[2], G. Hasemann[3], M. Krüger[3], B. Gorr[4]

[1] Institute for Material Engineering, University of Siegen, Paul-Bonatz-Str. 9-11, 57076 Siegen, Germany

[2] Institute of Energy and Climate Research, Microstructure and Properties of Materials (IEK-2), Forschungszentrum Jülich GmbH, Leo-Brand-Str. 1, 52425 Jülich, Germany

[3] Institute of Materials and Joining Technology, Otto-von-Guericke Universität Magdeburg, Universitätsplatz 2, 39106 Magdeburg, Germany

[4] Institute for Applied Materials – Applied Materials Physics (IAM-AMP), Karlsruhe Institute of Technology (KIT), Hermann-von-Helmholtz-Platz 1, 76344 Eggenstein-Leopoldshafen, Germany

Abstract

Thermodynamic modelling is an effective approach to accelerate the development of novel materials such as V-based alloys. In the present work, the results of thermodynamic modelling of the ternary system V-Ti-B using the "CALculation of PHAse Diagrams" (CALPHAD) method are presented. The thermodynamic descriptions of the binary systems V-Ti, V-B, and Ti-B are based on available publications whereas thermodynamic parameters for the ternary system stem from the iterative approximation to the experimental investigations, which further serve for verifying the calculated phase diagram. Thus, eight different alloys in the compositional range of 10 to 40 at.% Ti and B were analyzed aiming at identifying the evolving phases. A set of thermodynamic parameters is proposed. The calculated isothermal phase diagram at 1673 K exhibits a high degree of agreement with the literature and experimental observations. In our further work, the thermodynamic data generated in this study will be useful to develop the quaternary V-Ti-Si-B system.

1. Introduction

It is well-known that the enhanced operation temperature of gas turbines would lead to an increase in their overall thermal performance [1]. Due to their attractive properties such as high solidus temperatures and often exceptional mechanical properties, refractory metal-based alloys may substitute the currently used Ni-based superalloys. For the latter, the operating

* Mustafa Yazlak, Universität Siegen, Paul-Bonatz Str. 9-11, 57076 Siegen
Tel.: +49 271 / 740 – 3422, mustafa.yazlak@uni-siegen.de

temperatures in gas turbines are very close to their solidus temperature, therefore, a notable increase in inlet gas temperature with these alloys cannot be expected [2]. Nowadays, several refractory metal-based systems, such as Nb- or Mo-based are currently under intensive investigations aiming at the practical implementation of such materials in high-temperature environments [1, 3].

Thermodynamic modelling is usually used to accelerate the development of novel high-temperature materials since phase equilibria at elevated temperatures are particularly important for them. For example, a deep understanding of phase equilibria and thermodynamic modelling has successfully contributed to the development of Mo-based alloys. Xiong et al. performed the thermodynamic assessment of the Mo-Nb-Ta refractory system [4]. For instance, materials using Mo, Nb, and Ta by the addition of Si form Si-rich phases which are widely used for their superheat resisting alloys due to the oxidation resistance and the high melting points [4, 5]. Aiming at the development of refractory alloys with moderate density, Yang et al. introduced Mo-Si-Ti alloys and proposed a thermodynamic description of this system [6] which was further pursued by Azim et al. who carried out thermodynamic calculations to understand the effect of Ti additions on the constitution of Mo-Si-(B)-Ti alloys [7]. It was found that some alloys containing body-centered cubic (bcc), Mo_5Si_3 (T1), and Mo_5SiB_2 (T2) phases show an improved oxidation behavior due to the formation of SiO_2-TiO_2 layers [7, 8]. These theoretical, i.e. thermodynamic modelling and experimental investigations on the Mo-Si-Ti system were identified by Obert et al. who observed a further improvement of the oxidation behavior of Mo-Si alloys if Ti content increases [9]. Moreover, these alloys possess an enhanced creep resistance and a substantially decreased density. The formation of titanium silicide Ti_5Si_3 was declared to be the main reason for such a significant enhancement in the alloy performance [8].

The V-Si-B system yields a notable similarity to the aforementioned Mo-Si-B system. The V-Si-B alloys are being studied by several research teams. The phase stability of the V-Si-B system was reported by Nowotny et al. and served as a reference for Nunes et al. to study the phase relations in this system at 1600°C [10, 11]. Krüger et al. investigated the mechanical properties of the V-Si-B system and showed that the selected alloys possess very attractive values of specific creep resistance in a temperature range of 900 – 1050°C [12]. Similarly to the Mo-Si system, V-based disilicides with stoichiometry $(V,M)Si_2$ (M= Ti or Cr) form in the V-Si system. These disilicides do not suffer from pesting and are able to form a protective SiO_2 layer indicating that the oxidation behavior of V-Si-based alloys can be adjusted by controlling the characteristics of the disilicides such as phase fraction, their size, and distribution in the matrix [13]. The above consideration implicates that the V-Si-B system can also be considered as a prospective candidate for applications at high temperatures [12].

In line with the Mo-Si-(B)-Ti alloys which exhibit improved mechanical properties, density, and oxidation behavior a similar positive effect may be anticipated in the case of V-based alloys. In our studies, the development of novel V-Ti-Si-B alloys should also be guided by thermodynamic modelling. The ternary V-Si-B database has been developed by our team. As thermodynamic modelling is based on extrapolation, the V-Ti-B system is necessary to extend the existing database V-Si-B and create a quaternary system V-Ti-Si-B.

The present work aims at the thermodynamic modelling of the ternary system V-Ti-B using the CALPHAD method and the software FactSage© to perform the thermodynamic calculations [14]. The results of this theoretical assessment will be experimentally validated by microstructural studies.

2. Phase equilibria in the V-Ti-B system

Unfortunately, only a few systems containing the modelling of vanadium-based alloys have been treated in literature [10, 11, 15 - 27]. The relevant outcomes of these studies will be presented in the following.

2.1. The V-Ti system

The binary V-Ti system was assessed by Murray who studied the solubility of V in Ti and gained experimental solidus data [15]. Further, a phase diagram was proposed with its stable phases (i) the liquid phase, (ii) the close-packed hexagonal (α) solid solution at temperatures below 1155 K, and (iii) the body-centered cubic (β) solid solution at temperatures above 1155 K. Rubtsov et al. [17] investigated the activity of V in the β-phase containing 10 to 20 wt.% V at 1023 K, 1073 K, and 1123 K. The authors considered the results as approximated only. Therefore, no thermodynamic data were developed for optimization.

Through the solidus data of Rudy [28], the α-boundary data of Adenstedt [19] and Molokanov [20] as well as the β-boundary data of Adenstedt [19] and Ermanis [21], the thermodynamic parameters for the liquid, the bcc, and the hcp phases were developed by Ghosh [22] and used in this work for the modelling of this binary system.

2.2. The B-V System

Nowotny et al. [10], as well as Rudy and Windisch [18] investigated the phase equilibria of the system B-V. The phase stabilities of intermetallic phases V_3B_2, VB, V_3B_4, and VB_2 seem to be identical in both studies. Rudy and Windisch [18] carried out additional thermal studies and adjusted the solidus-liquidus temperatures. Spear and Gilles [23] confirmed the existence of stable phases determined in [10] and [18] by X-ray diffraction (XRD). In addition, the phases V_5B_6 and V_2B_3 were detected in the equilibrated samples. Due to minor changes in the lattice parameters, the homogeneity range of these compounds is considered to be narrow [18, 23]. All authors reported the solubility of B in the bcc V [10, 18, 29] as well as the solubility of V in

the beta-rhombohedral B [18] as negligible. Later Spear and Liao [24] summarized the chemical invariant reaction data and proposed a phase diagram based on the experimental data. The binary B-V system was more recently re-evaluated by Nunes et al. [11], who implied a peritectic formation of V_5B_6. Lima et al. [30] developed the liquid phase data while re-investigating the invariant reactions of the system. Both authors [11, 30] propose the following modifications to the existing V-B phase diagram:

- liquid composition of
  - $L \leftrightarrow BCC + V_3B_2$ at 12 at%
  - $L + VB \leftrightarrow V_3B_2$ at 19 at%
  - $L \leftrightarrow VB_2 + B$ at 95 at% of B
- VB phase forms congruently
- peritectic reaction for the formation of V_5B_6
  - $L + V_3B_4 \leftrightarrow V_5B_6$
- new eutectic reaction
  - $L \leftrightarrow VB + V_5B_6$

Table 1 - Crystallographic data of the intermetallic phases of the V-B system [14].shows crystallographic data of the stable intermetallic phases published by Villars and Calvert [14].

Table 1 - Crystallographic data of the intermetallic phases of the V-B system [14].

Phase	Pearson Symbol	Space Group	Prototype
V_3B_2	tP10	*P4/mbm*	U_3Si_2
VB	oS8	*Cmcm*	TlI
V_5B_6	oS22	*Cmmm*	V_5B_6
V_3B_4	oI14	*Immm*	Ta_3B_4
V_2B_3	oS20	*Cmcm*	V_2B_3
VB_2	hP3	*P6/mmm*	AlB_2

The thermodynamic information on this system in the following literature relates to the enthalpy of formation of the vanadium borides. Spear et al. [31] studied the equilibrium state of the ternary V-B-N system as well as the mass-spectrometric enthalpy of vaporization of the vanadium borides. In comparison, Topor and Kleppa [27] used drop calorimetry at 1400 K to investigate the enthalpy of formation of the vanadium borides. The thermodynamic modelling was performed by Spear et al. [32] considering the reference energy of pure elements as zero. Recently, Pinto da Silva et al. [26] published a re-optimization of the thermodynamic modelling of the V-B system, which is used to model this binary system in this work.

2.3. The Ti-B System

The Ti-B system was reviewed earlier by Kaufman et al. [33], Murray et al. [16], Bätzner [34], and Ma et al. [35]. The results published in [33] and [16] include elder Gibbs energy data for the pure elements which were not used in the re-assessment recently done by Witusiewicz et al. [36]. Rather, the newer data from Dinsdale [37] served as the basement for the modelling of the higher order systems. In the work of Bätzner [34], the solution phases TiB and TiB_2 were assumed as stoichiometric compounds, although the homogeneity ranges 49-50 at% B [38] and 65.2-67.6 at% B [39, 40] were experimentally identified in TiB and TiB_2, respectively. The thermodynamic description of Ma et al. [35] is based on the same experimental data as in [16]. The liquid phase was modelled using the substitutional solution model. The α-Ti, β-Ti, TiB and TiB_2 phases were modelled as a two-sublattice model and the Ti_3B_4 phase was modelled as a stoichiometric phase. However, Witusiewicz et al. [36] could not reproduce the composition and temperature ranges of two-phase equilibria between the liquid phase and the β-Ti and boride phases. Due to some discrepancies in the calculations compared to the available literature, Witusiewicz et al. [36] did further investigations and optimizations of the thermodynamic data. In this work, the set of parameters elaborated by Witusiewicz et al. [36, 41] was used for the modelling of the ternary V-Ti-B system.

2.4. The V-Ti-B System

The first assessment of the ternary V-Ti-B system was done by Kuz'ma et al. [42]. Nearly the entire composition range of the system was covered by the investigation of 40 different alloys. The phase constitution after heat treatment at 1673 K was studied by X-ray diffractometry and metallography. It should be mentioned that neither V_2B_3 nor V_5B_6 were considered in the work performed by Kuz'ma [42]. In other studies, Tyrell and Koster [43] determined the lattice parameter of the $(Ti,V)B_2$ phase. Later, Enomoto [44] summed up the experimental thermodynamic data of the system and presented an isothermal section of the ternary phase diagram at 1673 K. As no thermodynamic modelling of the V-Ti-B system has been done so far, parameters for the system Mo-Ti-B reported in [41] were used in this work because of the strong similarity of both systems.

3. Experimental procedure

Eight different alloys were prepared to verify and validate the calculated phase diagram. The raw materials were weighed in form of vanadium turnings (purity: 99.7 wt%), titanium granules (purity: 99.8 wt%), and boron granules (purity: 99.0 wt%). The alloys were remelted 5 times using arc melting and 2 times levitation melting under an argon atmosphere. The material loss for all samples was negligible regarding their mass loss (less than 1.0 wt%). The as-cast alloys were sealed in a quartz glass tube under an argon atmosphere and heat treated

at 1673 K for 100 h. The chemical compositions of the alloys were measured by inductively coupled plasma-optical emission spectrometry (ICP-OES / iCap 7600). The nominal and the measured compositions are shown in Table 2. Before the metallographic characterization, the samples were embedded in a copper-containing resin, ground with SiC abrasive paper up to #4000 grit, and polished with 1 µm silicon suspension OPS. The phases were analyzed by applying the scanning electron microscope (SEM)/focused ion beam (FIB) FEI NanoLab 600 and using energy dispersive X-ray spectroscopy (EDS). Phase fractions were evaluated using the software ImageJ. The chemical composition of the phases was measured using EDS on 10 different positions for each phase and is presented as an average value. In addition, the phases were identified by X-ray diffraction (XRD) measurements using the PANalytical Empyrean device and a step size of 0.053 [°2θ].

Table 2 - Nominal and measured chemical compositions of the V-Ti-B alloys

Alloy	Chemical composition [at%]		
	V	Ti	B
V-32Ti-10B	57.88	31.83	10.30
V-38Ti-10B	52.91	38.75	8.34
V-42Ti-10B	48.93	42.86	8.21
V-23Ti-30B	44.83	22.05	33.12
V-34Ti-30B	31.59	31.59	36.54
V-40Ti-30B	27.94	37.88	34.17
V-10Ti-40B	50.35	9.95	39.71
V-40Ti-40B	18.94	37.71	43.35

4. Thermodynamic models

The Gibbs-free enthalpy of pure elements depending on temperature can be described as:

$$^0G_m^\varphi - H_i^{SER} = A + BT + CT\ln(T) + DT^2 + ET^3 + FT^{-1} \tag{1}$$

where H_i^{SER} is the enthalpy of the stable element i at 298.15 K.

For the description of different phases, compound energy formalism (CEF) is used. This formalism describes the thermodynamic properties of a phase by considering the existence of sublattices. Sundman and Agren [45] as well as Hillert [46] described the CEF in detail. The Gibbs energy for a phase ϕ, G_m^φ, can be expressed by the following equation:

$$G_m^\varphi = \sum_s n^s(1 - y_{va}^s)\sum_i x_i\,{}^0G_i^{stst} + \sum_{end}\Delta_f^0G_{end}^\varphi \Pi y_i^s + RT\sum_s n^s\sum_i y_i^s\ln(y_i^s) + {}^{EX}G_m^\varphi \tag{2}$$

which can also be written in a shorter form according to Hillert [46]:

$$G_m^\varphi = \sum_{end}{}^0G_{end}^\varphi \Pi y_i^s + RT\sum_s n^s\sum_i y_i^s\ln(y_i^s) + {}^{EX}G_m^\varphi \tag{3}$$

with

$$^0G_{end}^{\varphi} = \Delta_f^0 G_{end}^{\varphi} + \sum_i {}^0G_i^{stst} n^s$$

(4)

The symbols in the past equations are described as follows:

n^s is the stoichiometric coefficient of the sublattice "s";
y_{va}^s is the site fraction of a vacancy in the sublattice "s";
x_i is the mole fraction of the component "i" in the compound;
$^0G_i^{stst}$ is the Gibbs free energy of component "i" at standard state;
end is an array with "end-member compounds";
$\Delta_f^0 G_{end}^{\varphi}$ is the Gibbs free energy of the formation of an end-member of a phase;
y_i^s is the site fraction of component "i" on the sublattice "s";
$^{EX}G_m^{\varphi}$ is the excess Gibbs energy of the phase ϕ

The Redlich-Kister polynomials [47] define the excess term considering the following contributions:

$$^{EX}G_m^{\varphi} = {}^{bin}G_{ex} + {}^{ter}G_{ex}$$

(5)

where the binary excess contribution is calculated by:

$$^{bin}G_{ex} = \sum_i \sum_{j>i} x_i x_j I_{ij}$$

(6)

$$I_{ij} = {}^0L_{ij} + {}^1L_{ij}(x_i - x_j) + {}^2L_{ij}(x_i - x_j)^2 + \cdots$$

(7)

with L_{ij} being the binary excess parameter.

The ternary excess contribution is calculated by:

$$^{ter}G_{ex} = x_i x_j x_k I_{ijk}$$

(8)

$$I_{ijk} = x_i {}^iL_{ijk} + x_j {}^jL_{ijk} + x_k {}^kL_{ijk}$$

(9)

with L_{ijk} being the ternary excess parameter.

The excess parameters $^nL_{ij}^{\varphi}$ and $^nL_{ijk}^{\varphi}$ of a phase as well as the Gibbs energy of formation of any end members, $\Delta_f^0 G_{end}^{\varphi}$, are calculated according to equation (1). The coefficients A, B, and C correspond to variables, which can be adjusted for an optimization of the procedure [26].

4.1. Solution liquid phase

The liquid phase was modelled as a single sublattice solution of V, B, and Ti.

4.2. Solutions phases with multiple sublattices

All phases of the thermodynamic database were modelled as solution phases. The Gibbs energy for these phases can be calculated using the CEF equations (1) to (3).

The (V,B)-bcc phase model was adopted from Pinto da Silva et al. [26] and extended by Ti. The remaining phases TiB, VB, (Ti,V)B_2, V_3B_2, V_2B_3, V_3B_4, V_5B_6, and Ti_3B_4 were optimized by iterative approximation to the isothermal phase diagram at 1673 K proposed by Enomoto [44].

5. Results and discussion

In this work, a database V-Ti-B was created; the results of thermodynamic calculations will be shown below starting with the corresponding binary systems. Figure 1 demonstrates the calculated phase diagram of the V-Ti system, which is in good agreement with the phase diagram reported in [22].
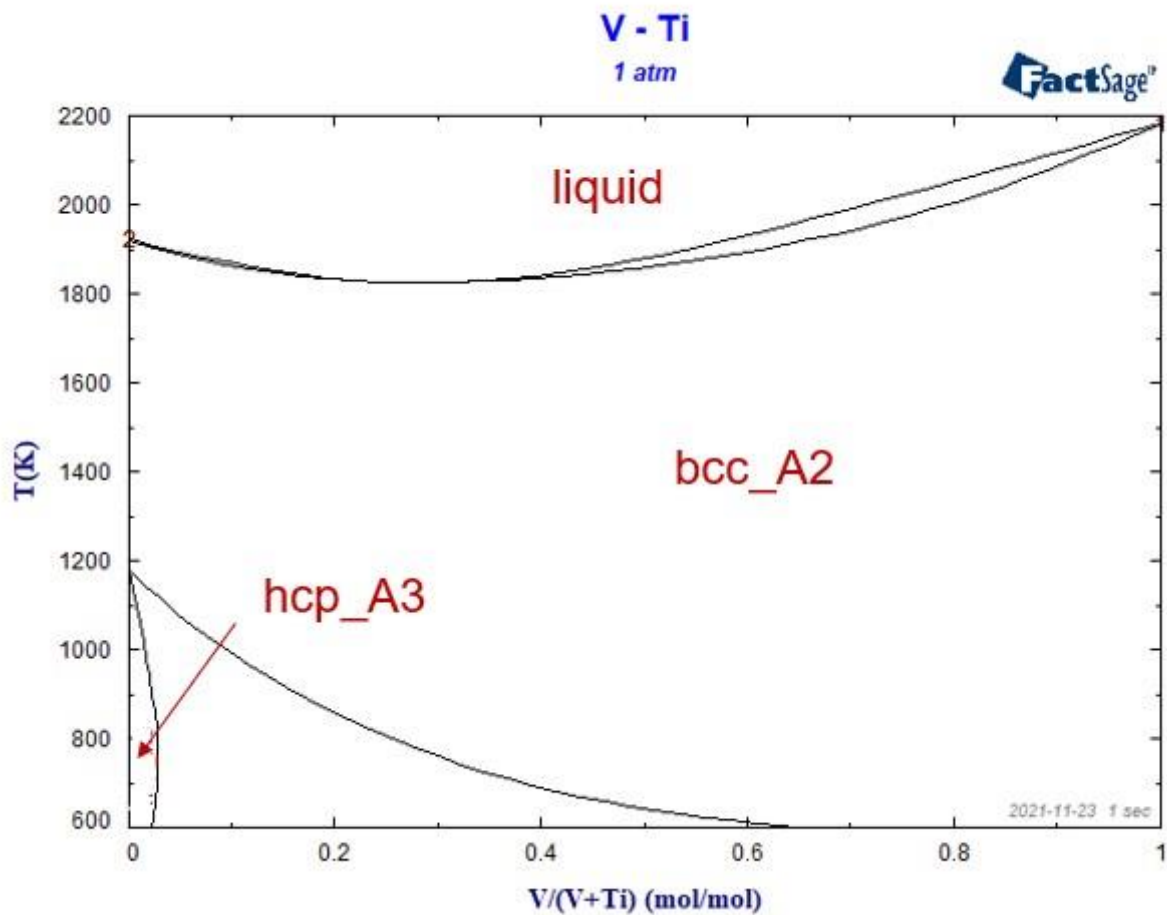

Figure 1: V-Ti phase diagram calculated using the thermodynamic data by Ghosh [22]

Figure 2 shows the calculated phase diagram of the binary system V-B based on the data published by Pinto da Silva et al. [26]. The database created in this work exhibits only negligible deviations compared to results found in the literature.
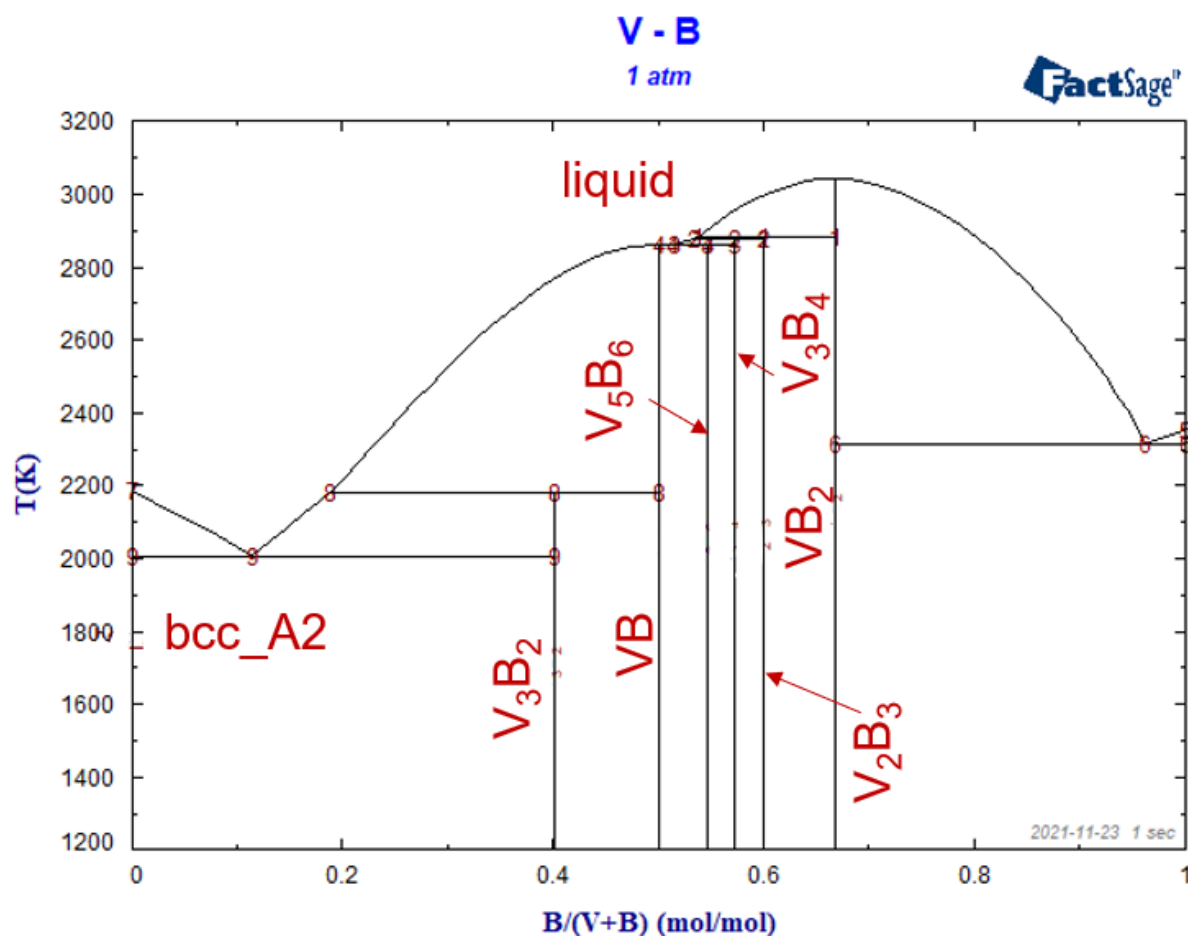

Figure 2: Calculated V-B phase diagram based on the thermodynamic data by Pinto da Silva et al. [26]

The phase diagram of the binary Ti-B system is shown in Fig. 3. The parameters were adapted from Witusiewicz et al. [36]. The according reactions are presented in the work of [36, 41]. The results in this work are in perfect agreement with the calculated data given in [36] and [41].
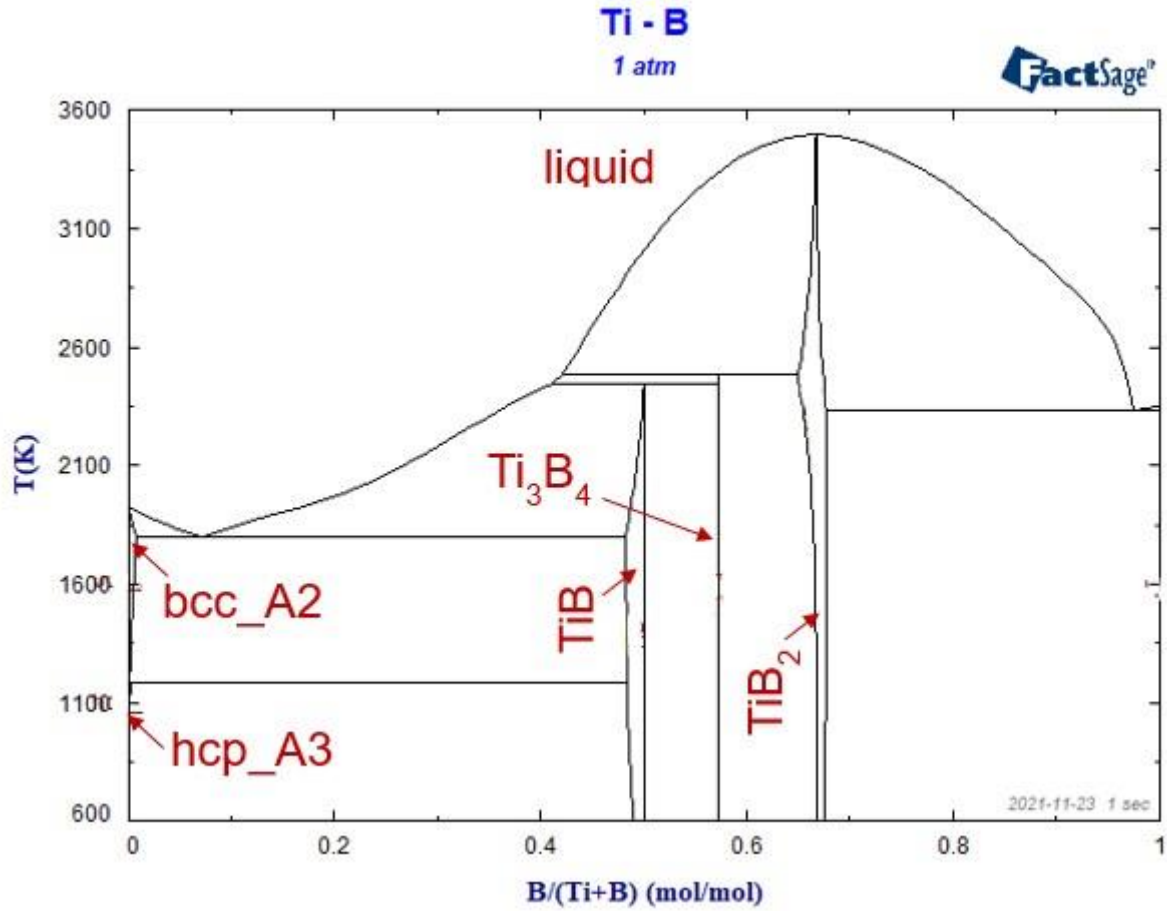
Figure 3: Ti-B phase diagram based on the thermodynamic data published in [36]

The developed thermodynamic database also shows a good agreement between the calculated ternary phase diagram of the V-Ti-B system and the isothermal phase diagram by Enomoto [44]. The optimized parameters representing coefficients of the Gibbs energy of each phase are listed in Table 3.

Table 3 – Optimized thermodynamic parameters for the ternary V-Ti-B system

Phase	Model	Parameter	Equation
bcc	$(V,Ti)_1(B,va)_3$	$^0G_{Ti:B}^{BCC}$	$^0G_{Ti}^{SER} + 3 * {}^0G_B^{SER} - 174000.24 - 34 * T$
		$^0L_{Ti:B,va}^{BCC}$	$-160162.96 + 30 * T$
TiB	$(Ti,V)_1(B,Ti,V)_1$	$^0L_{Ti:B,Ti}^{TiB}$	$-35924.76 + 24 * T$
VB	$(V,Ti,va)_{0.5}(B,va)_{0.5}$	$^0G_{V:B}^{VB}$	$0.5 * {}^0G_V^{SER} + 0.5 * {}^0G_B^{SER} - 55079.445 - 1.911 * T$
		$^0G_{Ti:B}^{VB}$	$0.5 * {}^0G_{Ti}^{SER} + 0.5 * {}^0G_B^{SER} - 50000$
		$^0G_{va:B}^{VB}$	$0.5 * {}^0G_B^{SER} + 28579$
		$^0G_{V:va}^{VB}$	$0.5 * {}^0G_V^{SER} + 88805$
		$^0G_{Ti:va}^{VB}$	$0.5 * {}^0G_{Ti}^{SER} + 25000$
		$^0G_{va:va}^{VB}$	$-4108.4 * T$
		$^0L_{V,Ti:B}^{TiB}$	$-195770 + 17 * T$
		$^1L_{V,Ti:B}^{TiB}$	-5000

		$^0L_{V:B,va}^{TiB}$	-90000
(Ti,V)B$_2$	(B,V,Ti)$_1$(B,V,Ti)$_2$	$^0G_{B:B}^{(Ti,V)B_2}$	$3 * {}^0G_B^{SER} + 79628$
		$^0G_{B:V}^{(Ti,V)B_2}$	$^0G_B^{SER} + 2 * {}^0G_V^{SER} - 29580$
		$^0G_{V:B}^{(Ti,V)B_2}$	$2 * {}^0G_B^{SER} + {}^0G_V^{SER} - 138325 - 12.281 * T$
		$^0G_{V:V}^{(Ti,V)B_2}$	$3 * {}^0G_V^{SER} + 165000$
		$^0G_{Ti:B}^{(Ti,V)B_2}$	$-360600 + 1.865 * T + 1.2547 * T * \ln(T)$ $+ 3.131 * 10^{-3} * T^2 - 4.105 * 10^{-7} * T^3$
		$^0G_{Ti:V}^{(Ti,V)B_2}$	$^0G_{Ti}^{SER} + 2 * {}^0G_V^{SER} + 65000$
		$^0G_{V:Ti}^{(Ti,V)B_2}$	$^0G_V^{SER} + 2 * {}^0G_{Ti}^{SER} + 65000$
		$^0L_{B:B,Ti}^{TiB}$	98091
		$^0L_{Ti:B,Ti}^{TiB}$	98091
		$^0L_{B,Ti:B}^{TiB}$	$-103672.21 + 30 * T$
		$^0L_{B,Ti:Ti}^{TiB}$	$-103672.21 + 30 * T$
		$^0L_{B,V:B}^{TiB}$	$-103672.21 + 30 * T$
		$^0L_{B,V:V}^{TiB}$	$-103672.21 + 30 * T$
		$^0L_{V,Ti:B}^{TiB}$	$246400 - 236 * T + 0.0538 * T^2$
		$^1L_{V,Ti:B}^{TiB}$	$-81315 + 34.26 * T$
V$_3$B$_2$	(V,Ti,va)$_{0.6}$(B,va)$_{0.4}$	$^0G_{Ti:B}^{V_3B_2}$	$0.6 * {}^0G_{Ti}^{SER} + 0.4 * {}^0G_B^{SER} - 1000$
		$^0G_{va:B}^{V_3B_2}$	$0.4 * {}^0G_B^{SER} + 28579$
		$^0G_{V:va}^{V_3B_2}$	$0.6 * {}^0G_V^{SER} + 71805$
		$^0G_{Ti:va}^{V_3B_2}$	$0.6 * {}^0G_{Ti}^{SER} + 10000$
		$^0G_{va:va}^{V_3B_2}$	$-1108.4 * T$
		$^0L_{V,Ti:B}^{V_3B_2}$	$-169970 + 14 * T$
		$^1L_{V,Ti:B}^{V_3B_2}$	-49500
		$^0L_{V:B,va}^{V_3B_2}$	-75000
V$_2$B$_3$	(V,Ti,va)$_{0.4}$(B,va)$_{0.6}$	$^0G_{Ti:B}^{V_2B_3}$	$0.4 * {}^0G_{Ti}^{SER} + 0.6 * {}^0G_B^{SER} - 25000$
		$^0G_{V:B}^{V_2B_3}$	$0.6 * {}^0G_B^{SER} + 0.4 * {}^0G_V^{SER} - 48079.445 - 2 * T$
		$^0G_{va:B}^{V_2B_3}$	$0.6 * {}^0G_B^{SER} + 28579$
		$^0G_{V:va}^{V_2B_3}$	$0.4 * {}^0G_V^{SER} + 88805$
		$^0G_{Ti:va}^{V_2B_3}$	$0.4 * {}^0G_{Ti}^{SER} + 10000$
		$^0G_{va:va}^{V_2B_3}$	$-3108.4 * T$
		$^0L_{V:B,va}^{V_2B_3}$	-75000
		$^0L_{V,Ti:B}^{V_2B_3}$	$-109970 + 17 * T$
V$_3$B$_4$	(V,Ti,va)$_{0.43}$(B,va)$_{0.57}$	$^0G_{Ti:B}^{V_3B_4}$	$0.43 * {}^0G_{Ti}^{SER} + 0.57 * {}^0G_B^{SER} - 25000$
		$^0G_{V:B}^{V_3B_4}$	$0.57 * {}^0G_B^{SER} + 0.43 * {}^0G_V^{SER} - 50379.445 - 2 * T$
		$^0G_{va:B}^{V_3B_4}$	$0.57 * {}^0G_B^{SER} + 28579$
		$^0G_{V:va}^{V_3B_4}$	$0.43 * {}^0G_V^{SER} + 88805$
		$^0G_{Ti:va}^{V_3B_4}$	$0.43 * {}^0G_{Ti}^{SER} + 10000$

		$^0G_{va:va}^{V_3B_4}$	$-3108.4*T$
		$^0L_{V:B,va}^{V_3B_4}$	-75000
V_5B_6	$(V,Ti,va)_{0.4545}(B,va)_{0.5455}$	$^0G_{Ti:B}^{V_5B_6}$	$0.4545*{}^0G_{Ti}^{SER}+0.5455*{}^0G_B^{SER}-25000$
		$^0G_{V:B}^{V_5B_6}$	$0.5455*{}^0G_B^{SER}+0.4545*{}^0G_V^{SER}-52179.445-2*T$
		$^0G_{va:B}^{V_5B_6}$	$0.5455*{}^0G_B^{SER}+28579$
		$^0G_{V:va}^{V_5B_6}$	$0.4545*{}^0G_V^{SER}+88805$
		$^0G_{Ti:va}^{V_5B_6}$	$0.4545*{}^0G_{Ti}^{SER}+10000$
		$^0G_{va:va}^{V_5B_6}$	$-3108.4*T$
Ti_3B_4	$(V,Ti)_3(B)_4$	$^0G_{Ti:B}^{Ti_3B_4}$	$GTiB+GTiB2-85422.850-0.717*T-0.14*T*\ln(T)$ $+0.00074T^2$
		$^0G_{V:B}^{Ti_3B_4}$	$4*{}^0G_B^{SER}+3*{}^0G_V^{SER}$
		$^0L_{V,Ti:B}^{Ti_3B_4}$	$-538733+92*T$
		$^1L_{V,Ti:B}^{Ti_3B_4}$	174130

Figure 4 represents the calculated ternary phase diagram of the V-Ti-B system as compared with the corresponding diagram published in ref. [44]. In general, the phase diagram calculated in this work bears a striking resemblance with that constructed by Enomoto [44] in the V- and Ti-rich regions, while distinctive deviations are visible if B content is between 50 at.% and 70 at.%. In particular, the quantitative differences between the experimentally determined values and calculated phase fractions for all alloys (see Table 2) are shown in Table 4. Most of the calculated phase fractions show a reasonable agreement with the corresponding experimental values. The majority of the occurring differences are below or around 10 %. Nevertheless, a few significant discrepancies were also identified. The calculations of the phase equilibria of the alloy V-42Ti-10B reveal two stable phases. However, three phases, i.e., bcc, TiB, and V_3B_2 phases were experimentally detected. The alloy V-34Ti-30B shows higher amounts of the TiB and the bcc phases in the calculations. It is assumed, that the reason for this inaccuracy is due to the lack of reliable data between the ranges of the two-phase field bcc + TiB and the three-phase field bcc + TiB + V_3B_2. Regarding the experimental results, the three-phase field bcc + TiB + V_3B_2 seems to have a higher range than proposed by Enomoto [44]. These results reveal that the stability ranges of the two-phase field bcc + TiB and the three-phase field bcc + TiB + V_3B_2 still need further investigations and optimizations to reach a higher degree of accuracy.
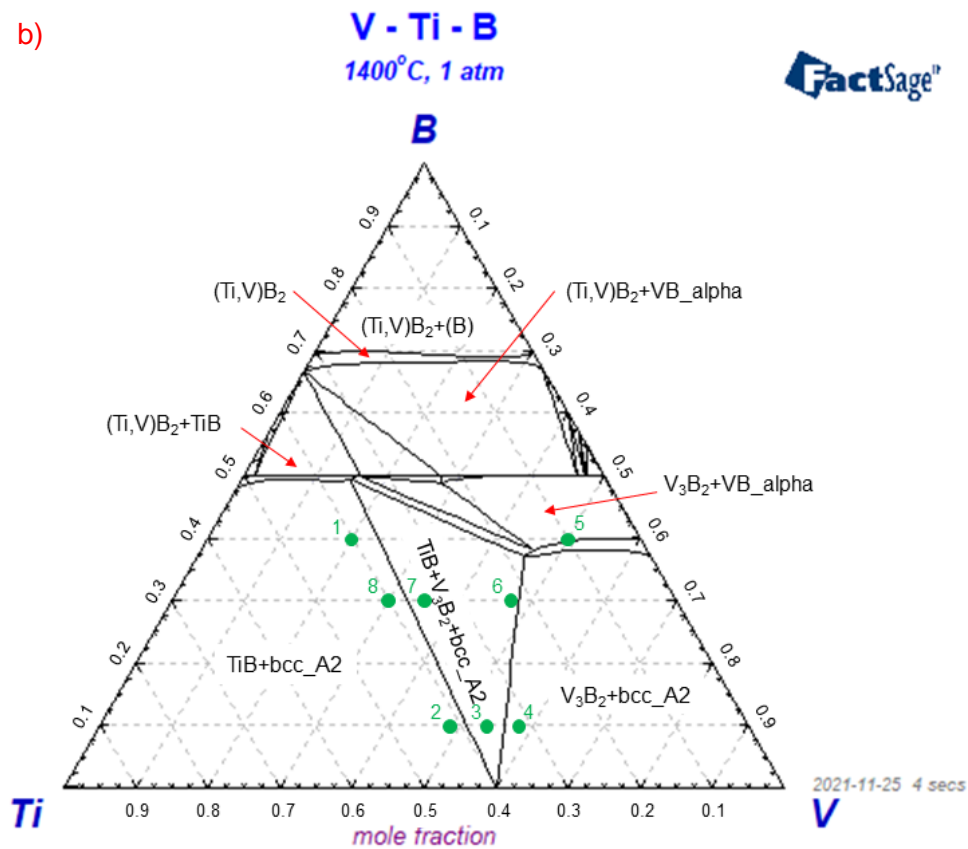
a)
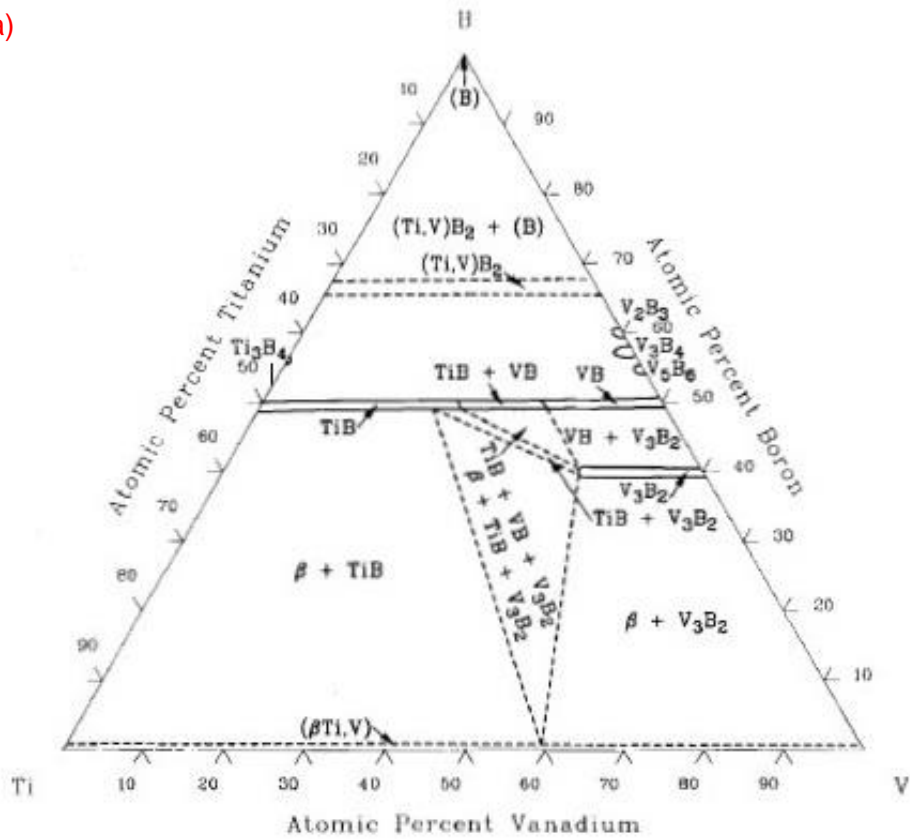
b)

Figure 4: Comparison of the isothermal section of the V-Ti-B phase diagram at 1673K; (a) literature data [44] and (b) phase diagram calculated in this work (experimentally investigated alloys are marked green)

Table 4 - Accuracy of calculated phase fractions in comparison to data derived from micrographs of cross-sections

Nr.	Alloy	Phase	Experimental [%]	Calculated [%]	Difference [%]	
1	V-40Ti-40B	bcc	22.03	22.21	-	0.18
		TiB	77.97	77.79	+	0.18
2	V-42Ti-10B	bcc	69.04	83.05	-	14.01
		TiB	18.73	16.95	+	1.78
		V_3B_2	12.23	-	+	12.23
3	V-38Ti-10B	bcc	67.74	82.12	-	14.38
		TiB	13.91	13.61	+	0.30
		V_3B_2	18.35	4.27	+	14.08
4	V-32Ti-10B	bcc	71.71	78.06	-	6.35
		V_3B_2	28.29	21.94	+	6.35
5	V-10Ti-40B	V_3B_2	89.07	99.78	-	10.71
		VB	10.93	0.22	+	10.71
6	V-23Ti-30B	bcc	20.45	25.32	-	4.87
		TiB	9.33	4.53	+	4.80
		V_3B_2	70.22	70.15	+	0.07
7	V-34Ti-30B	bcc	18.49	40.52	-	22.03
		TiB	14.34	44.40	-	30.06
		V_3B_2	67.17	15.08	+	52.09
8	V-40Ti-30B	bcc	37.86	44.48	-	6.62
		TiB	62.14	55.52	+	6.62

Figs. 5 (a) and (b) show the microstructure of selective alloys V-42Ti-10B and V-34Ti-30B to be located in the three-phase equilibria area bcc + TiB + V_3B_2. These alloys were chosen to verify the calculated phase boundary between the three-phase field bcc + TiB + V_3B_2 and the two-phase field bcc + TiB. As shown in Fig. 5, both alloys seem to exhibit three phases, namely bcc, TiB, and V_3B_2. The measured compositions of TiB, V_3B_2 and the bcc phase are summarized in Table 5. As EDX data for boron are unreliable Table 5 shows the measured metal components recalculated under the assumption of ideal B-contents.

Table 5 – Measured metal components (EDX) of phases in the annealed samples at 1400°C for 100h recalculated with assumed stoichiometric ideal B-contents

Nominal alloy composition	Phases	Composition (at.%)		
		V	Ti	B
V-42Ti-10B	TiB	6.75	43.25	50.00
	V_3B_2	54.78	5.22	40.00
	V_{bcc}	70.55	29.45	-
V-34Ti-30B	TiB	6.44	43.56	50.00
	V_3B_2	51.94	8.06	40.00
	V_{bcc}	76.14	23.86	-
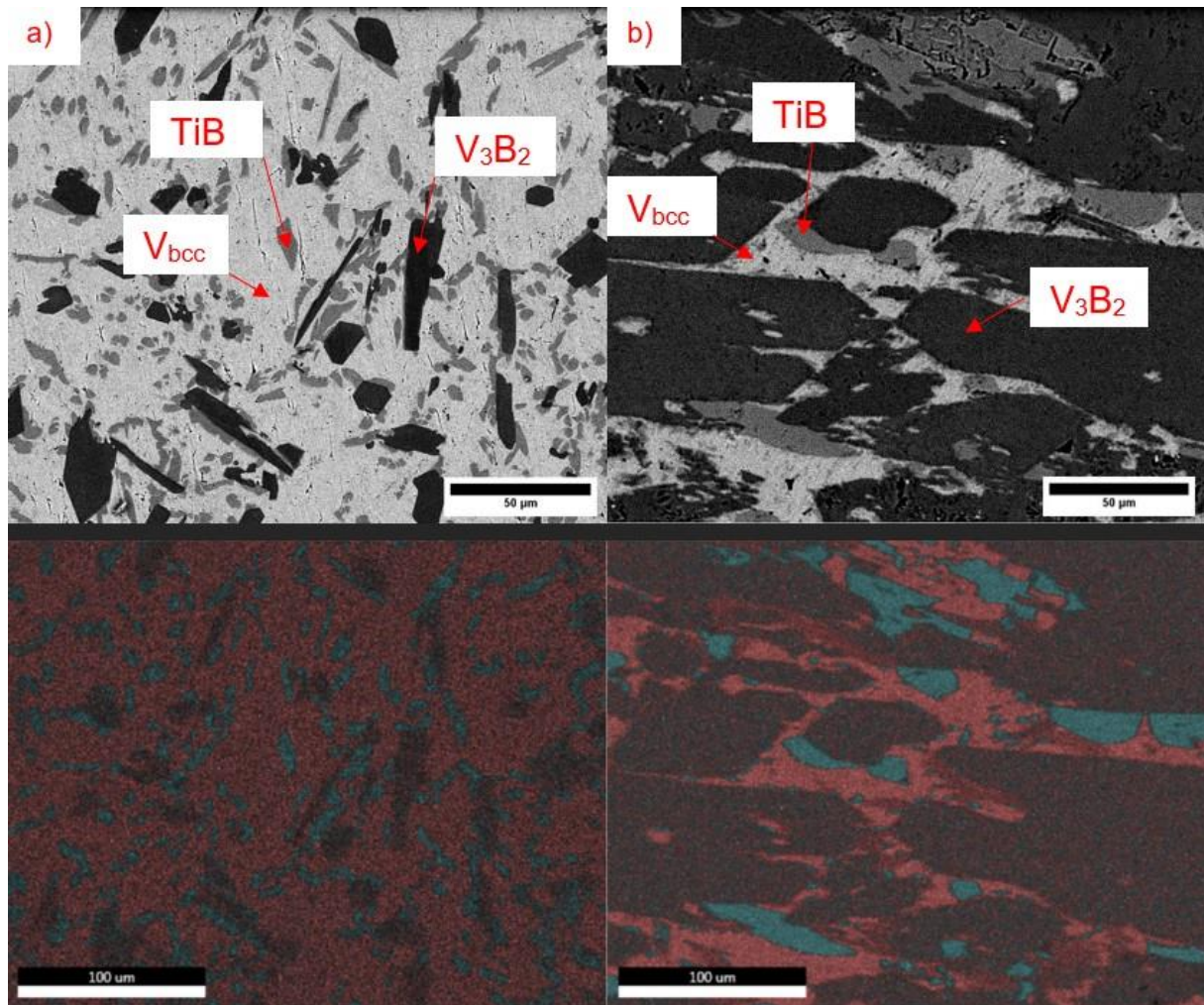
Figure 5: SEM-BSE and EDS micrographs of (a) V-42Ti-10B and (b) V-34Ti-30B alloys after annealing at 1673K/100h (red: V-content; aqua: Ti-content)

For further identification of the phases, an XRD scan was performed. The XRD pattern is presented in Fig. 6 and reveals reflexes that can be attributed to an A2-type crystal structure of the bcc phase, a B27-type crystal structure of the TiB phase, and a D5$_a$-type crystal structure of the V_3B_2 phase. The XRD pattern proves the assumption that both alloys belong to the three-phase field bcc + TiB + V_3B_2.
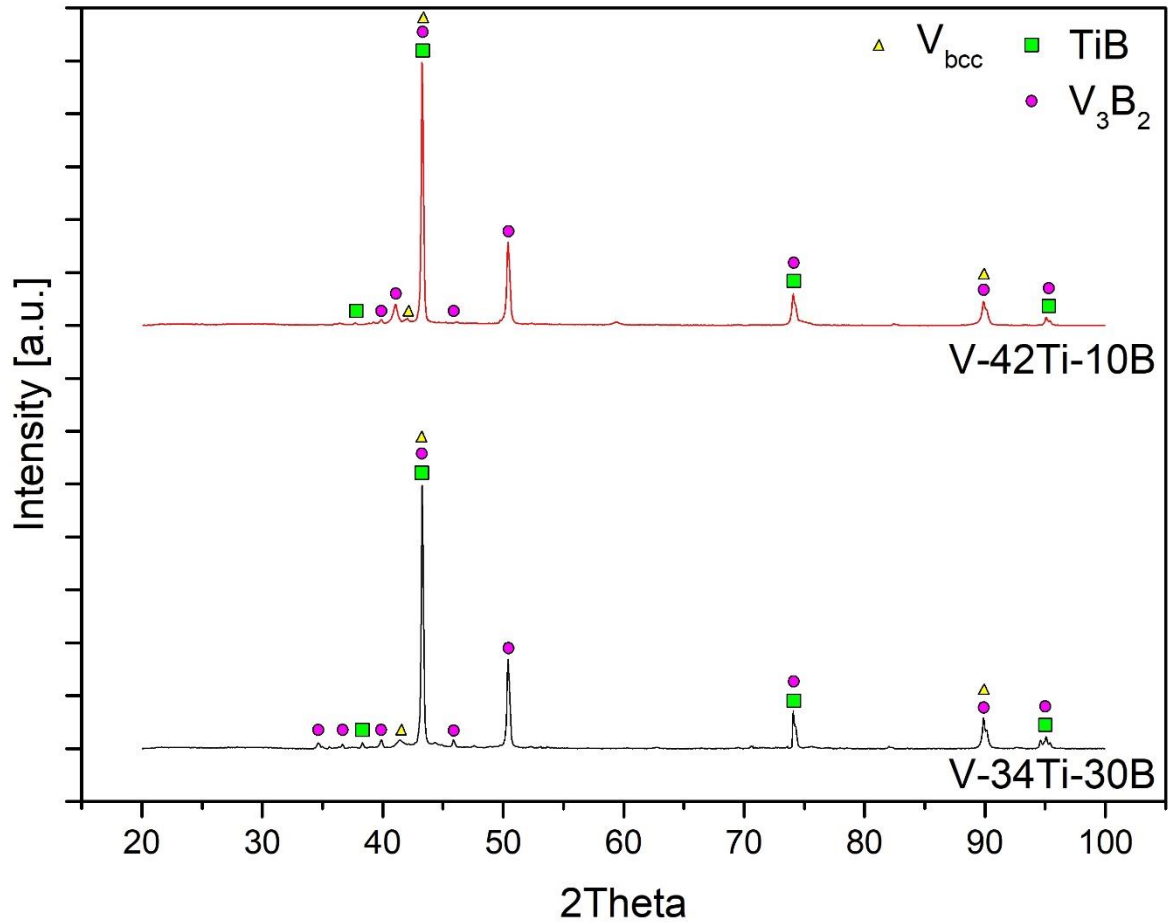
Figure 6: XRD-diffractograms of the alloys V-42Ti-10B and V-34Ti-30B

Our future studies will concentrate on (i) improvement of the V-Ti-B database and (ii) thermodynamic calculations, in particular, of liquidus projections of V-Ti-B alloys. As shown in the results, the three-phase equilibria area bcc + TiB + V_3B_2 needs further research regarding the phase boundaries. In addition, the calculation of the liquidus projection relies on further investigations of the reaction temperatures of the system. The improvement of the database is essential for the creation of the mentioned V-Ti-Si-B system.

Summary

Refractory metal-based materials such as V-based alloys have been considered to be an efficient substitution for widely used Ni-based superalloys. The V-Ti-Si-B system seems to be especially attractive due to its prospective specific mechanical properties. To accelerate the alloy development, it is aimed at the creation of a V-Si-B-Ti database. In this work, a database for the ternary V-Ti-B system – as part of the V-Si-B-Ti system – was developed and the results of thermodynamic calculations were experimentally validated. While all binary systems show excellent agreement with literature data, some deviations were identified in V-Ti-B alloys with the B concentrations between 50 and 70 at.%. It resulted, that both investigated alloys are located in the three-phase equilibria area bcc + TiB + V_3B_2, consequently, there is further optimization necessary to reach higher accuracy. Our future investigations will be concentrated on the improvement of the database V-Ti-B and the creation of further binary and ternary sub-systems for the quaternary V-Si-B-Ti system.

References

[1] Harada, H.: High Temperature materials for gas turbines: The present and future. In: Proceedings of the International Gas Turbine Congress. Tokyo 2003

[2] Pollock, T. M.,Tin, S.: Nickel-based superalloys for advanced turbine engines: chemistry, microstructure and properties. Journal of Propulsion and Power 22 (2006), p. 361–374

[3] Heilmaier, M., Krüger, M., Saage, H., Rösler, J., Mukherji, D., Glatzel, U., Völkl, R., Hüttner, R., Eggeler, G., Somsen, C., Depka, T., Christ, H.-J., Gorr, B.,Burk, S.: Metallic materials for structural applications beyond nickel-based superalloys. Journal of the minerals 61 (2009), p. 61–67

[4] Xiong, W., Du, Y., Liu, Y., Huang, B. Y., Xu, H. H., Chen, H. L.,Pan, Z.: Thermodynamic assessment of the Mo–Nb–Ta system. Calphad 28 (2004), p. 133–140

[5] Bewlay, B. P., Jackson, M. R., Subramanian, P. R.,Zhao, J.-C.: A review of very-high-temperature Nb-silicide-based composites. Metallurgical and Materials Transactions A 34 (2003), p. 2043–2052

[6] Yang, Y., Chang, Y. A., Tan, L.,Du, Y.: Experimental investigation and thermodynamic descriptions of the Mo–Si–Ti system. Materials Science and Engineering: A 361 (2003), p. 281–293

[7] Azim, M. A., Burk, S., Gorr, B., Christ, H.-J., Schliephake, D., Heilmaier, M., Bornemann, R.,Bolívar, P. H.: Effect of Ti (Macro-) alloying on the High-Temperature oxidation behavior of ternary Mo–Si–B Alloys at 820–1,300 °C. Oxidation of Metals 80 (2013), p. 231–242

[8] Azim, M. A., Schliephake, D., Hochmuth, C., Gorr, B., Christ, H.-J., Glatzel, U.,Heilmaier, M.: Creep resistance and oxidation behavior of novel Mo-Si-B-Ti Alloys. Journal of the minerals 67 (2015), p. 2621–2628

[9] Obert, S., Kauffmann, A., Seils, S., Schellert, S., Weber, M., Gorr, B., Christ, H.-J.,Heilmaier, M.: On the chemical and microstructural requirements for the pesting-resistance of Mo–Si–Ti alloys. Journal of Materials Research and Technology 9 (2020), p. 8556–8567

[10] Nowotny, H., Benesovsky, F.,Kieffer, R.: Contribution to the structure of the Vanadium-Boron system. Zeitschrift für Metallkunde 50 (1959), p. 258–261

[11] Nunes, C. A., Lima, B. B., Coelho, G. C., Rogl, P.,Suzuki, P. A.: On the stability of the V5B6-phase. Journal of Alloys and Compounds 370 (2004), p. 164–168

[12] Krüger, M., Bolbut, V., Gang, F.,Hasemann, G.: Microstructure variations and creep properties of novel high temperature V-Si-B materials. Journal of the minerals 68 (2016), p. 2811–2816

[13] Chaia, N., Bouizi, Y., Mathieu, S.,Vilasi, M.: Isothermal and cyclic oxidation behaviour of hot-pressed MSi2 compounds (with M = V, Ti, Cr). Intermetallics 65 (2015), p. 35–41

[14] Villars, P.,Calvert, L. D.: Pearson's Handbook of Crystallographic Data for Intermediate Phases. American Society of Materials 1985

[15] Murray, J. L.: The Ti−V (Titanium-Vanadium) system. Bulletin of Alloy Phase Diagrams 2 (1981), p. 48–55

[16] Murray, J. L., Liao, P. K.,Spear, K. E.: Phase diagrams of binary titanium alloys. ASM International 2 (1987), p. 340–345

[17] Rubtsov, A. N., Olesov, Y. G., Cherkashin, V. I.,Suchkov, A. B.: Activity of aluminum, vanadium and chromium in binary alloys with titanium. Russian Metallurgy 6 (1970), p. 56–58

[18] Rudy, E.,Windisch, S.: Related binary systems. Part I, systems VB, Nb-B and Ta-B. In: Ternary phase equilibria in transition metal-boron-carbon-silicon systems. 1966, p. 1–104

[19] Adenstedt, H. K., Pequignot, J. R.,Raymer, J. M.: The Titanium-Vanadium system. Transactions ASM 44 (1952), p. 990–1003

[20] Molokanov, V. V., Chernov, D. B.,Budberg, P. B.: Solubility of vanadium in α-titanium. Metal Science and Heat Treatment 19 (1977), p. 704–705

[21] Ermanis, F., Farrar, P. A.,Margolin, H.: A reinvestigation of the systems Ti-Cr and Ti-V. Transactions AIME 221 (1961), p. 904–908

[22] Ghosh, G.: Thermodynamic and kinetic modeling of the Cr-Ti-V system. Journal of Phase Equilibria 23 (2002), p. 310–328

[23] Spear, K. E.,Gilles, P. W.: Phase and structure relationships in the vanadium-boron system. High Temperature Sciences 1 (1969), p. 86–97

[24] Spear, K. E., Liao, P. K.,Smith, J. F.: The B−V (Boron-Vanadium) system. Journal of Phase Equilibria 8 (1987), p. 447–454

[25] Lima, J. A. S.: Cosmologia, quintessência e aceleração do universo. Journal of Phase Equilibria (2004) 62, p. 134–139

[26] Pinto da Silva, A. A. A., Chaia, N., Ferreira, F., Carvalho Coelho, G., Fiorani, J.-M., David, N., Vilasi, M.,Nunes, C. A.: Thermodynamic modeling of the V-Si-B system. Calphad 59 (2017), p. 199–206

[27] Topor, L.,Kleppa, O. J.: Enthalpies of formation of first-row transition-metal diborides by a new calorimetric method. The Journal of Chemical Thermodynamics 17 (1985), p. 1003–1016

[28] Rudy, E.: Compendium of phase diagram data. Wright-Patterson Air Force Base Ohio: Air Force Materials Laboratory Metals and Ceramics Division 1969

[29] Rostoker, W.,Yamamoto, A.: A survey of Vanadium binary systems. Transactions ASM 46 (1954), p. 1136–1167

[30] Lima, B. B., Nunes, C. A., Coelho, G. C., Suzuki, P. A.,Rogl, P.: Evaluation of the invariant reactions of the V-B System. Journal of Phase Equilibria & Diffusion 25 (2004), p. 134–139

[31] Thermodynamics of the Vanadium Borides. Kansas Univ., Lawrence. Dept. of Chemistry CONF-670935-3; COO-1140-164, Spear, K. E., Schaefer, H.,Gilles, P. W., Butterworths, London 1969

[32] Spear, K. E., Blanks, J. H.,Wang, M. S.: Thermodynamic modeling of the V-B system. Journal of the Less Common Metals 82 (1981), p. 237–243

[33] Kaufman, L., Uhrenius, B., Birnie, D.,Taylor, K.: Coupled pair potential, thermochemical and phase diagram data for transition metal binary systems-VII. Calphad 8 (1984), p. 25–66

[34] Bätzner, C.: System B-Ti. In: Ansara, I., Dinsdale A. T.a. Rand, M. R. (Eds.): Thermochemical database for light metal alloys. 1998, p. 129–132

[35] Ma, X., Li, C., Du, Z.,Zhang, W.: Thermodynamic assessment of the Ti–B system. Journal of Alloys and Compounds 370 (2004), p. 149–158

[36] Witusiewicz, V. T., Bondar, A. A., Hecht, U., Rex, S.,Velikanova, T.: The Al–B–Nb–Ti system. Journal of Alloys and Compounds 448 (2008), p. 185–194

[37] Dinsdale, A. T.: SGTE data for pure elements. Calphad 15 (1991), p. 317–425

[38] Fenish, R. G.: Phase relationships in the Titanium-Boron system. NRM-138 138 (1964), p. 1–37

[39] Ternary phase equilibria in transition metal-boron-carbon-silicon systems. Part 5. Compendium of phase diagram data. Air Force Materials Laboratory Technical Report AFML-TR 5-2, Part V, Rudy, E., Ohio 1969

[40] Thebault, J., Pailler, R., Bontemps-Moley, G., Bourdeau, M.,Naslain, R.: Chemical compatibility in boron fiber-titanium composite materials. Journal of the Less Common Metals 47 (1976), p. 221–233

[41] Witusiewicz, V. T., Bondar, A. A., Hecht, U., Potazhevska, O. A.,Velikanova, T.: Thermodynamic modelling of the ternary B–Mo–Ti system with refined B–Mo description. Journal of Alloys and Compounds 655 (2016), p. 336–352

[42] Kuz'ma, Y. B., Paitash, T. P.,Baidala, S. I.: Phase equilibria in the Ti-V-B and Ti-Mn-B systems. Vestn. L'vov Univ. 11 (1969), p. 18–20

[43] Tyrrell, M. E.,Koster, J.: Preparation and Evaluation of the diborides $(Ti,V)B_2$, $(Ti,Nb)B_2$ and $(Ti,Ta)B_2$. U.S. Bureau Mines Report Investigation 6407 (1964), p. 1–16

[44] Enomoto, M.: The B-Ti-V system. Journal of Phase Equilibria 13 (1992), p. 641–644

[45] Sundman, B.,Ågren, J.: A regular solution model for phases with several components and sublattices, suitable for computer applications. Journal of Physics and Chemistry of Solids 42 (1981), p. 297–301

[46] Hillert, M.: The compound energy formalism. Journal of Alloys and Compounds 320 (2001), p. 161–176

[47] Redlich, O.,Kister, A. T.: Algebraic representation of thermodynamic properties and the classification of solutions. Industrial & Engineering Chemistry 40 (1948), p. 345–348